이학석사 학위논문

The PRR-EC-SWR1 complex shapes diurnal hypocotyl growth by modulating *PIF4* expression

PRR-EC-SWR1 복합체의 *PIF4* 조절에 의한 일주기적 하배축 생장 조절

2022 년 8 월

서울대학교 대학원

화학부 생화학 전공

원 진 훈

The PRR-EC-SWR1 complex shapes diurnal hypocotyl growth by modulating *PIF4* expression

지도 교수 서 필 준

이 논문을 이학석사 학위논문으로 제출함

2022 년 8 월

서울대학교 대학원

화학부 생화학 전공

원 진 훈

원진훈의 이학석사 학위논문을 인준함

2022 년 6 월

위 원 장 이 현 우 (인)

부위원장 서 필 준 (인)

위 원 오 은 규 (인)

ABSTRACT

The PRR-EC-SWR1 complex shapes diurnal hypocotyl growth by modulating *PIF4* expression

Jin Hoon Won
Department of Chemistry
College of Natural Science
Seoul National University

The circadian clock entrained by environmental light cycles allows plants to fine-tune diurnal responses, such as growth, development, and defense against biotic and abiotic challenges. Here, I show that physical interactions among the evening-expressed clock components, including PSEUDO-RESPONSE REGULATOR5 (PRR5), TIMING OF CAB EXPRESSION1 (TOC1), and the Evening Complex (EC) component EARLY FLOWERING 3 (ELF3), define diurnal repressive domain at the *PHYTOCHROME INTERACTING FACTOR4* (*PIF4*) locus for rhythmic hypocotyl growth. The three genes act synergistically to gate hypocotyl growth at nighttime as the rhythmic growth rate dramatically shifts in *prr5 toc1 elf3* mutants with a substantial increase in *PIF4* expression. Notably, transcriptional repression of *PIF4* by the PRR5, TOC1, and ELF3 proteins involves the chromatin remodeling SWI2/SNF2-RELATED (SWR1) complex to incorporate H2A.Z at the *PIF4* locus during the night. Overall, these findings indicate that the PRRs-EC-

SWR1 module shapes diurnal hypocotyl growth through a distinctive epigenetic mechanism.

Keyword: Hypocotyl growth**,** Circadian clock, PRR, Evening complex (EC), H2A.Z, SWR1 complex, PIF4

Student Number: 2019-22185

CONTENTS

1. INTRODUCTION

1.1. Study Background

Plants have evolved to maintain an internal rhythm with a period of 24 h. Light and temperature cycles are the major environmental cues that shape the circadian clock. Then, the circadian clock ensures timely responses, including growth, stress response, and metabolism (Bonnot and Nagel, 2021; Covington and Harmer, 2007; Seo and Mas, 2015; Steed et al., 2021), in synchronization with diurnal environmental changes. The representative study model for circadian regulation of plant growth is diurnal hypocotyl elongation. The rhythmic hypocotyl growth of *Arabidopsis* is intricately shaped by the diurnally-regulated PHYTOCHROME-INTERACTING FACTOR (PIF) basic helix-loop-helix (bHLH) transcription factors, which promote cell elongation through the activation of auxin biosynthesis and signaling-related genes (Gray William et al., 1998; Sun et al., 2012), as well as brassinosteroids biosynthesis genes (Martínez et al., 2018; Oh et al., 2012).

The PIF activities are regulated at multiple regulatory layers, allowing them to be active mainly at the nighttime. Plant red/far-red photoreceptor PHYTOCHROME B (phyB) is converted from inactive Pr form into active Pfr form under light exposure during the day, which is translocated into the nucleus (Klose et al., 2015) and interacts with PIF4 protein. The interaction between active phyB (Pfr) and PIFs facilitates phosphorylation of PIF proteins, leading to PIF degradation (Huq and Quail, 2002; Lorrain et al., 2008). Meanwhile, under dark conditions, phyB is sequestered in the cytoplasm after reversion into inactive Pr form, which results in rhythmic PIF4 accumulation at night (Huq and Quail, 2002; Lorrain et al., 2008).

A majority of core clock components either bind to *PIF* loci or interact with the PIF proteins to gate their activities specifically at nighttime (Li et al., 2020; Liu et al., 2013; Martín et al., 2018; Nakamichi et al., 2012; Niwa et al., 2009; Nohales et al., 2019; Zhu et al., 2016). The *Arabidopsis* PSEUDO RESPONSE REGULATORs (PRRs) family consists of five members (PRR9, PRR7, PRR5, PRR3, and TIMING OF CAB EXPRESSION 1 [TOC1]), and they share considerable numbers of target genes, including *PIF*s (Martín et al., 2018; Soy et al., 2016; Zhu et al., 2016). The PRR9 and PRR7 directly bind to the *PIF4* and *PIF5* promoters for transcriptional repression (Liu et al., 2013; Nakamichi et al., 2012) during daytime, and PRR5 and TOC1 subsequently repress *PIF* expression during evening time, allowing *PIF*s to be upregulated temporally at end of night. TOC1 also physically interacts with PIF3 and PIF4 and antagonistically regulates growth-promoting genes including *CYCLING DOF FACTOR 5* (*CDF5*), *PHYTOCHROME INTERACTING FACTOR3-LIKE 1* (*PIL1*), and *LONG HYPOCOTYL IN FAR-RED* (*HFR1*) to further shape PIF activities (Martín et al., 2018; Soy et al., 2016). In addition, the Evening Complex (EC) composed of three circadian components, EARLY FLOWERING 3 (ELF3), ELF4, and LUX ARRHYTHMO (LUX), which peak at dusk (Doyle et al., 2002; Hazen et al., 2005; Hicks et al., 2001; Liu et al., 2001; Nusinow et al., 2011; Onai and Ishiura, 2005), is also known to integrate circadian signals into *PIF4* and *PIF5* for diurnal growth regulation (Box et al., 2015; Lu et al., 2012; Murcia et al., 2022; Nomoto et al., 2012; Nusinow et al., 2011). The LUX protein recruits ELF3 and ELF4 at *PIF4* and *PIF5* loci at evening time for their transcriptional repression (Silva et al., 2020). Moreover, protein-protein interaction of ELF3 with PIFs interferes with target DNA binding activity of PIFs in an EC-independent manner (Nieto et al., 2015).

Overall, PIF4 and PIF5 activities are repressed from morning to evening through the combined effects mentioned above, and gated mainly at late nighttime.

The EC involves epigenetic mechanisms in the regulation of target gene expression, especially circadian-regulated genes. Indeed, the EC interacts with multiple chromatin modifiers such as HISTONE DEACETYLASE 9 (HDA9) and Jumonji C domain-containing histone demethylase JUMONJI 29 (JMJ29) (Lee and Seo, 2021; Lee et al., 2019; Park et al., 2019). In addition, the EC also works with SWI2/SNF2-RELATED 1 (SWR1) chromatin remodeling complex, which include PHOTOPERIOD INDEPENDENT EARLY FLOWERING 1 (PIE1), ACTIN-RELATED PROTEIN 6 (ARP6), and SERRATED LEAVES AND EARLY FLOWERING (SEF/SWC6) (Aslam et al., 2019; Lei and Berger, 2020; March-Díaz and Reyes, 2009), to exchange canonical H2A into histone variant H2A.Z, thus establishing robust transcriptional repressive domain at target gene loci. Enrichment of H2A.Z is primarily observed in the gene body region to be transcriptionally silenced (Coleman-Derr and Zilberman, 2012; Kumar, 2018; Lei and Berger, 2020), and furthermore, global H2A.Z deposition occurs diurnally and mediates circadian-dependent gene expression control (Tong et al., 2020). For example, H2A.Z deposition is enriched at EC-targeted morning genes *PRR9* and *PRR7* around dusk (Tong et al., 2020).

1.2. Purpose of Research

Although circadian components are supposed to act synergistically in the control of rhythmic plant responses (Li et al., 2020), a precise mechanism of how the main circadian proteins work together to control rhythmic plant growth. Here, I demonstrate that the circadian core oscillators PRR5, TOC1, and ELF3 interact

with each other and synergistically regulate *PIF4* expression and thereby diurnal hypocotyl elongation. Notably, the PRR-EC complex further recruits SWR1 complex, forming a robust transcriptional repressive complex. Overall, my study reveals that the core circadian complex facilitates robust evening responses via repressive chromatin domains.

2. MATERIALS AND METHODS

2.1 Plant materials and growth conditions

Arabidopsis thaliana ecotype Columbia (Col-0) was used for all experiments. Plants were grown under neutral-day (ND) conditions (12h light/12h dark) using cool white fluorescent lamps (150 μmol photons m^{-2} s^{-1}) at 22°C. The *prr5-1*, *toc1-21*, *elf3-1*, *prr5-1 toc1-21*, *prr5-1 elf3-1*, *toc1-21 elf3-1*, *prr5-1 toc1-21 elf3-1*, *arp6-1*, and *sef-1* seedlings were previously described (Deal et al., 2005; Ding et al., 2007; Ezer et al., 2017; Li et al., 2020; March-DíAz et al., 2007; Wang et al., 2010). The *ELF3:ELF3-MYC/elf3-1*, *TMG-YFP* (*TOC1:TOC1-YFP*), *PRR5:PRR5-eGFP*, PRR5-ox, PRR5-ox/*elf3-1*, TOC1-ox, TOC1-ox/*elf3-1* were previously described (Ezer et al., 2017; Li et al., 2020; Más et al., 2003; Nakamichi et al., 2012; Yamashino et al., 2003).

2.2 Hypocotyl length measurement

Sterilized seeds were sown on 1/2 Murashige and Skoog (MS) medium supplemented with 0.75% (w/v) agar and 1% (w/v) sucrose. After stratification at 4 °C for 3 days, plants were grown vertically under 22 °C ND conditions for 7 days. Seedlings were photographed after incubation for 7 days, and hypocotyl lengths were measured by using Image J software (http://rsb.info.nih.gov/ij).

For hypocotyl growth rate measurement, seedlings were grown at 22 °C ND condition for 8 days and photographed every 3 hours under near-infrared light (λ=850nm). Hypocotyl lengths were measured after 1 day incubation in 22°C ND, at the onset of seeds germination. Hypocotyl lengths were measured with Image J software and growth rates were calculated from length differences divided by the

time interval (3h) between subsequent images. For daytime and nighttime growth rate comparison, the length differences between ZT0 and ZT12 (or ZT12 and ZT24) were divided by the time interval (12h).

2.3 Bioinformatics analysis

The genome browser at iRegNet (Shim et al., 2021) was used for confirmation of direct binding of circadian components to the *PIF4* locus (GSE36361, GSE35953, and GSE137264) and H2A.Z deposition in *elf3-1*, *arp6*, and *pie1* (GSE109101, GSE108450, and GSE139459) .

H2A.Z ChIP-seq data was downloaded from National Center for Biotechnology Information Gene Expression Omnibus under accession number GSE109101 (Tong et al., 2020). ChIP-seq reads were trimmed using Trim-Galore (v0.6.7) (https://www.bioinformatics.babraham.ac.uk/projects/trim_galore/) and mapped using Bowtie2 (v2.4.5) (Langmead and Salzberg, 2012) with default parameters. MACS2 (v2.2.7.1) (Zhang et al., 2008) was used for calculating the fold enrichment (IP/input) of mapped reads. PRR5 target genes, TOC1 target genes and EC target genes were obtained from previous studies (Huang et al., 2012; Nakamichi et al., 2012; Tong et al., 2020). A set of random genes were selected from Araport11 annotated genes. The selected genes overlapped with other sets were excluded. H2A.Z enrichment profiles of target genes were drawn using DeepTools (Ramírez et al., 2016).

2.4 ChIP-qPCR analysis

ChIP assays were conducted with seedlings grown under 22 °C ND for 2 weeks. Whole seedlings were harvested at the indicated time (ZT4 or ZT16) and

crosslinked in PBS (pH 7.4) containing 1% formaldehyde (BIOPURE, 4920F) for 15 min under vacuum. Frozen seedlings were ground in nuclei lysis buffer (50 mM Tris-HCl, 10 mM EDTA, 1% SDS, 1 mM PMSF, and 1X protease inhibitor cocktail [Roche], pH 8.0) and solubilized chromatin was ultrasonicated at 4°C for 20 cycles (30s ON and 30s OFF, full power) to approximately 500 bp fragments using a Bioruptor Pico (Diagenode). Fragmented chromatin was incubated with anti-H2A.Z (abcam, ab4174) or anti-MYC (Millipore, 05-724) at 4 °C overnight followed by incubation with 25 µl of Protein A (Dynabeads, 10001D) or Protein G magnetic beads (Dynabeads 10003D) respectively. To immunoprecipitate GFP and YFP epitopes, fragmented chromatin was incubated with 25 µl of anti-GFP magnetic agarose (Chromotek, gtma-20) at 4 °C for overnight. Beads were washed with low salt buffer (20mM Tris, 2mM EDTA, 0.2% SDS, 0.5% Triton X-100, 150mM NaCl, 1X protease inhibitor cocktail, pH 8.0), high salt buffer (20mM Tris, 2mM EDTA, 0.2% SDS, 0.5% Triton X-100, 500mM NaCl, 1X protease inhibitor cocktail, pH 8.0), LiCl buffer (10mM Tris, 1mM EDTA, 0.5% Nonidet P-40, 0.5% sodium deoxycholate, 250mM LiCl, 1X protease inhibitor cocktail, pH 8.0), and twice with TE buffer (10mM Tris, 1mM EDTA, 0.1% Triton X-100, pH 8.0). Chromatin was eluted in 500 µl of elution buffer (1% SDS, 0.1M $NaHCO_3$) and reverse-crosslinked for overnight at 65°C. After Proteinase K treatment (Biopure, 7730P), DNA fragments were purified by phenol/chloroform extraction and quantified by quantitative real-time PCR (qRT-PCR). Values for control plants were set to 1 after normalization against *eIF4a* for qPCR analysis.

2.5 RT-qPCR analysis

Seeds were sown on 1/2 MS medium supplemented with 0.75% (w/v) agar and 1%

(w/v) sucrose and grown under 22°C ND conditions for 2 weeks. Whole plants were harvested at the indicated time. To extract total RNA, samples were ground in liquid nitrogen, and 1ml TransZol Up (Transgen Biotech, ET111-01) was mixed thoroughly with the ground tissue. After centrifugation at 12,000g for 10 min at 4°C, the supernatant was transferred to new Eppendorf tube. 250 µl chloroform was added, and RNA in the aqueous phase was precipitated with isopropanol. The RNA pellet was washed twice with 70% ethanol and dissolved in RNase-free deionized water. 2 µg RNA was treated with DNase I (New England Biolabs, M0303L), followed by reverse transcription using the M-MLV reverse transcriptase (MG MED, MR01601). RT-qPCR was performed in 96-well blocks on the Step-One Plus Real-Time PCR System (Applied Biosystems) using sequence-specific primers and SYBR Master MIX (Enzynomics, RT501M). The expression of each gene was normalized relative to the *EUKARYOTIC TRANSLATION INITIATION FACTOR 4A1* (*eIF4a*) gene (At3g13920). All RT-qPCR reactions were performed using cDNA synthesized from total RNA extracted from independent biological triplicates. Relative expression level was calculated using ΔΔ Ct method. The Ct value of each reaction was determined automatically by the system using default parameters. The specificity of RT-qPCR reactions was determined by melt curve analysis of the amplified products using the standard method installed in the system.

2.6 Transient expression assays using Arabidopsis protoplasts

For effector plasmid construction, cDNA fragments of *PRR5*, *TOC1* and ELF3 were cloned into pEarleygate201 vector and pEarleygate203 vector via Gibson assembly cloning method (Gibson et al., 2009). For reporter plasmid construction, upstream ~2,052 bp promoter sequence of *PIF4* and whole *PIF4* genomic DNA

sequence were cloned into modified pCAMBIA1305 vector containing a minimal cauliflower mosaic virus (CaMV) 35S promoter and the *β-glucuronidase* (*GUS*) gene. A plasmid with *firefly luciferase* (*LUC*) gene driven by 35S promoter was co-transfected as an internal control for quantification of transfection efficiency.

Protoplast isolation and DNA transfection were performed as previously described with minor modifications (Yoo et al., 2007). Briefly, mesophyll protoplasts were isolated from 3-week-old Arabidopsis seedlings grown under 22°C ND condition. 20 μg of each effector, reporter and internal control plasmid were co-transfected into 1.2 x 10^6 protoplasts by PEG-mediated plasmid transfection. After 16-24 hours incubation in W5 medium in dark at 22 °C, GUS and LUC activities were measured at ZT16 using Tristar2 LB942 Multimode Microplate Reader (Berthold Technologies).

2.7 Yeast two-hybrid (Y2H) assays

Y2H assays were performed using the BD Matchmaker system (Clontech). cDNA fragments of *PRR5*, *TOC1*, *ELF3*, *ARP6*, *SEF*, *PIE1* (535-825) and *PIE1* (1670-1730) were subcloned into the pGBKT7 or pGADT7 vectors to generate GAL4 activation domain (AD) and GAL4 DNA-binding domain (BD) fusion constructs. Full length GAL4 transcription factor was expressed as a positive control. The GAL4 AD and BD constructs were co-transformed into the yeast strain pJG69-4A harboring the *LacZ* and *His* reporter genes, and the transformed cells were selected by growth on synthetic defined (SD) medium lacking leucine and tryptophan (SD/-Leu/-Trp), and SD medium lacking Leu, Trp, histidine, and adenine (SD/-Leu/-Trp/-His/-Ade).

2.8 Bimolecular fluorescence complementation (BiFC) assays

For BiFC assays, coding sequence of *PRR5* and *TOC1* were cloned into pSAT4-nEYFP-N1 (E3083) to produce C-terminal in-frame fusion with N-terminal 173 amino acid of YFP (nYFP) to produce PRR5-nYFP and TOC1-nYFP construct respectively. Full length *ELF3* coding sequence was inserted in pSAT4-cEYFP-C1-B (E3082) for N-terminal in-frame fusion with C-terminal 68 amino acid of YFP (cYFP) to produce cYFP-ELF3 construct. The recombinant constructs were co-transfected with nuclear marker (mCherry-NLS) into *Arabidopsis* protoplasts. After incubation for 16 hours in 22 °C dark, protoplasts were observed using CQ1 confocal quantitative image cytometer (Yokogawa).

2.9 CoIP assays using Arabidopsis protoplasts

For protein expression in *Arabidopsis* protoplasts, coding sequences of PRR5, TOC1, ELF3, and sequence containing the SANT domain of PIE1 (1469-1984) were cloned into pEarleygate201 (HA-tag), pEarleygate202 (FLAG-tag) and pEarleygate203 (MYC-tag) plasmid vectors. The 60 µg of each recombinant plasmids were transfected into 3.6 x 10^6 protoplasts by PEG-mediated plasmid transfection. After incubation in dark for 16-24 hours, protoplasts expressing recombinant proteins were harvested in cold IP lysis buffer (50mM Tris, 1mM EDTA, 150mM NaCl, 10% glycerol, 0.5% Triton X-100, 1X protease inhibitor cocktail, pH 7.5) and incubated in ice for 15 minutes. Total lysates were briefly sonicated for nucleus disruption at 4°C for 3 cycles (30s ON and 30s OFF). After centrifugation at 12,000 rpm for 20 minutes, supernatants were incubated with either 25 µl of Pierce anti-HA magnetic beads (Thermo, 88837), or anti-FLAG M2 magnetic beads (Sigma, M8823). After incubation for overnight at 4°C, beads were

washed 3 times with IP wash buffer (50mM Tris, 1mM EDTA, 150mM NaCl, 10% glycerol, 0.1% Triton X-100, 1X protease inhibitor cocktail, pH 7.5). The immunoprecipitated fractions were eluted using acid elution buffer (100mM glycine, pH 2.5), subsequently treated with neutralization buffer (1.5M Tris-HCl, pH 8.8). An adequate amount of 5x SDS loading buffer was added, then boiled for 5 minutes at 100 °C. The immune complexes were analyzed by western blot using anti-HA antibody (Millipore, 05-904), anti-FLAG M2 antibody (Sigma, F1804), and anti-MYC antibody (Millipore, 05-724).

2.10 Split luciferase assays

For split luciferase assays, coding sequences of PRR5, TOC1, and ELF3 were cloned into pGWB-nLUC (1-416 amino acids of firefly luciferase), while C-terminal coding region of PIE1 (1469-1984) was inserted into pGWB-cLUC (398-550 amino acids of firefly luciferase) vector. The recombinant constructs were co-transfected to *Arabidopsis* protoplasts. GUS overexpressing plasmids were used as internal control for measuring transfection efficiency. In addition, effector plasmids overexpressing HA-PRR5, HA-TOC1, or MYC-ELF3 were transfected to confirm the synergistic effect. After incubation under 22°C dark for 16-24 hours, protoplasts were resuspended in imaging solution (W5 medium containing 2mM D-luciferin) for luciferase activity measurement. Subsequently, protoplasts were lysed for GUS activity measurement.

3. RESULTS

3.1. Synergistic hypocotyl growth repression by PRR5, TOC1 and ELF3.

PRR5, TOC1, and ELF3 are known to regulate hypocotyl elongation through controlling *PIF* expression (Kaczorowski and Quail, 2003; Martín et al., 2018; Nieto et al., 2015; Nusinow et al., 2011; Sato et al., 2002; Soy et al., 2016; Yamamoto et al., 2003; Zhu et al., 2016). In addition, expression of *PRR5*, *TOC1* and EC components temporally coincides in a day, which are active during evening time (Figure 1), suggesting that they may work together and are sophisticated in the control of diurnal growth. To examine the association of their function in diurnal hypocotyl growth, hypocotyl lengths of *prr5*, *toc1*, *elf3* single mutants as well as high-order mutants were measured. Hypocotyl lengths of *toc1-21* and *elf3-1* mutants were increased by by 2- and 4-fold, respectively, compared with wild type (Figure 2A and 2B). *prr5-1* mutant also displayed marginally but reproducibly increased hypocotyl (Figure 2A and 2B). Notably, hypocotyl lengths of *prr5-1 toc1-21*, *prr5-1 elf3-1*, *toc1-21 elf3-1* and *prr5-1 toc1-21 elf3-1* mutants were significantly increased compared with their corresponding single mutants (Figure 2A and 2B), as previously reported (Li et al., 2020).

3.2 PRR5, TOC1 and ELF3 repress hypocotyl growth specifically at night.

Based on the overlapping expression of *PRR5*, *TOC1*, and *ELF3* that peak during evening (Figure 1), I suspected that increased hypocotyl elongation of the high-order mutants was caused by derepression of growth inhibition during nighttime. Indeed, hypocotyl growth rate measurement using time-lapse imaging showed that

hypocotyl elongation of *prr5-1 toc1-21*, *prr5-1 elf3-1*, *toc1-21 elf3-1* and *prr5-1 toc1-21 elf3-1* mutants was promoted specifically during nighttime, as shown in *prr5*, *toc1*, *elf3* single mutants (Figure 2C and Figure 3), while hypocotyl growth rate of all examined mutants was indistinguishable to wild type during daytime (Figure 2C and Figure 3). Consistently, nighttime growth rates were proportional to overall hypocotyl lengths (Figure 2A to 2C), indicating that PRR5, TOC1, and ELF3 work together to gate hypocotyl elongation at nighttime.

3.3 PIF4 is co-targeted by PRR5, TOC1 and ELF3 during nighttime.

To investigate how PRR5, TOC1, and ELF3 co-regulate diurnal hypocotyl growth, I obtained chromatin immunoprecipitation sequencing (ChIP-seq) datasets conducted using PRR5, TOC1, and ELF3-epitope tagged plants (Huang et al., 2012; Nakamichi et al., 2012; Tong et al., 2020) and identified genes co-targeted by the three proteins. Among the 7 candidate genes, I focused on *PIF4* (Figure 4A, Table 1), which functions as a hub integrating light signals and temperature cues into plant growth program and promotes diurnal hypocotyl growth via increased auxin biosynthesis (Koini et al., 2009; Sun et al., 2012; Zhao and Bao, 2021). In support, PRRs and ELF3 were bound to the same chromatin regions of the *PIF4* promoter (Figure 4B). The overlapping binding sites contained both G-box motif (CACGTG, -660 bp) (Gendron et al., 2012) and LUX-binding site (LBS, GATTCG, -376 bp) (Helfer et al., 2011), which are known as *cis*-elements bound by PRRs and the EC, respectively. ChIP-qPCR analysis using *PRR5:PRR5-eGFP*, *TMG-YFP* (*TOC1:TOC1-YFP*), and *ELF3:ELF3-MYC/elf3-1* transgenic plants also revealed that they were targeted to the similar regions of the *PIF4* promoter (Figure 5A to 5C), and their binding occurred simultaneously at dusk (Figure 1).

3.4 Synergistic nighttime repression of PIF4 is mediated by PRR5, TOC1 and ELF3.

I next examined whether *PIF4* expression is co-regulated by PRR5, TOC1, and ELF3. Diurnal expression of *PIF4* was analyzed in *prr5-1*, *toc1-21*, and *elf3-1* single and *prr5-1 toc1-21*, *prr5-1 elf3-1*, *toc1-21 elf3-1* and *prr5-1 toc1-21 elf3-1* high-order mutants by quantitative real-time RT-PCR (RT-qPCR) analysis. Although transcript accumulation of *PIF4* was negligibly influenced in *prr5-1*, *toc1-21*, *prr5-1 toc1-21*, and *elf3-1* mutants at ZT4 and ZT8, *PIF4* expression during the nighttime was increased in proportion to the extent of hypocotyl elongation and night-time growth rate (Figure 6 and Figure 7A). Furthermore, *PIF4* expression was more strikingly increased at nighttime in *prr5-1 elf3-1*, *toc1-21 elf3-1*, and *prr5-1 toc1-21 elf3-1* high-order mutants (Figure 6 and Figure 7A), consistent with the nighttime hypocotyl growth rate of each mutant (Figure 2C and Figure 3). It was notable that *PIF4* transcription was synergistically regulated by PRR5, TOC1, and ELF3, as *PIF4* expression at ZT16 was dramatically elevated in high-order mutants (*prr5-1*/Col-0, 1.51-fold; *toc1-21*/Col-0, 4.91-fold; *prr5-1 toc1-21*/Col-0, 16.7-fold; *elf3-1*/Col-0, 83.2-fold; *prr5-1 elf3-1*/Col-0, 139.0-fold; *toc1-21 elf3-1*/Col-0, 108.3-fold; *prr5-1 toc1-21 elf3-1*/Col-0, 304.2-fold) (Figure 7A).

To confirm the synergistic function of PRRs and ELF3 in regulating *PIF4* expression, I generated the *pPIF4:gPIF4-GUS* reporter construct, in which genomic sequence of *PIF4* covering 2,052 bp-upstream promoter and genic regions was fused in-frame to β-glucuronidase (GUS)-encoding sequence, and the reporter construct was co-transfected with the effector construct overexpressing *PRR5*, or *ELF3* (*35S:HA-PRR5*, or *35S:MYC-ELF3*). The *PIF4* expression was repressed in protoplasts overexpressing PRR5, or ELF3 (Figure 7B). Notably, PRR5 and TOC1

were synergistic in *PIF4* repression, as well as mutual overexpression of PRRs and ELF3 synergistically repressed *PIF4* gene (Figure 7B). Overall, these results indicate that PRRs and ELF3 bind to the *PIF4* promoter at dusk and synergistically repress its transcription at the nighttime.

3.5 Formation of PRRs-ELF3 complex.

Based on the overlapping binding sites of PRR5, TOC1 and ELF3 at the *PIF4* locus as well as their synergistic functions in *PIF4* repression in the control of hypocotyl elongation, the key circadian components were supposed to form protein complex at dusk. Yeast two-hybrid assays (Y2H) showed that PRR5 physically interacts with ELF3 and TOC1 *in vitro* (Figure 8A). To further support the interactions between PRRs and EC *in vivo*, I conducted bimolecular fluorescence complementation (BiFC) assays using *Arabidopsis* protoplasts. The coding sequences of *PRR5* and *TOC1* were fused to the sequence encoding N-terminal half of the yellow fluorescent protein (nYFP), and the coding sequence of *ELF3* was fused in-frame to C-terminal half of YFP (cYFP). Strong YFP signals were observed in the nucleus of *Arabidopsis* protoplast co-expressing the combinations of PRR5-nYFP/cYFP-ELF3 and TOC1-nYFP/cYFP-ELF3, while no detectable signals were observed in protoplasts expressing negative controls (Figure 8B). I also performed co-immunoprecipitation (Co-IP) assays using *Arabidopsis* protoplasts transiently expressing 35S:*HA-PRR5*, *HA-TOC1* and 35S:*MYC-ELF3*. Protoplasts were harvested at ZT16 to verify the interaction at dusk. The HA-PRR5 and HA-TOC1 protein was immunoprecipitated and subjected with immunoblot analysis using anti-MYC antibody (Figure 8C). As a result, I confirmed that PRR5 and TOC1 also associated with EC *in planta*. Together, these results indicate that

PRR5, TOC1, and the EC assemble into a protein complex at dusk.

3.6 PRRs require ELF3 for hypocotyl repression.

I next asked whether PRRs and ELF3 are required for each other to regulate *PIF* expression and thereby hypocotyl elongation. To this end, I measured hypocotyl lengths of transgenic plants overexpressing PRR5 and TOC1 in Col-0 and *elf3-1* mutant background. Overexpression of *PRR5* significantly reduced hypocotyl elongation with lower *PIF4* expression in wild-type background, but impact of *PRR5* overexpression disappeared in *elf3-1* mutant background (Figures 9A, 9B and 11A). The hypocotyl length and the *PIF4* expression of *PRR5-ox/elf3-1* was equivalent to that of *elf3-1* (Figures 9A, 9B and 11A). Hypocotyl growth rate measurement also supported that both *PRR5-ox/elf3-1* and *elf3-1* seedlings exhibited a comparable growth rate during nighttime (Figure 9C and Figure 10). Similarly, the TOC1 function in diurnal hypocotyl elongation was also dependent on ELF3. The reduced overall hypocotyl length, nighttime growth rate, and the *PIF4* expression displayed in *TOC1-ox* was significantly compromised in *TOC1-ox/elf3-1* (Figures 9A to 9C, Figure 10, and Figure 11A), suggesting that PRR function is dependent on ELF3 in the control of diurnal *PIF4* expression and hypocotyl elongation.

To confirm whether PRRs and ELF3 are interdependent each other in the *PIF4* repression, I transiently expressed an effector construct overexpressing *PRR5*, *TOC1*, or *ELF3*, along with *pPIF4:gPIF4-GUS* reporter construct, in protoplasts isolated from wild-type, *elf3-1*, and *prr5-1 toc1-21* seedlings. GUS activity measurement revealed that *PIF4* expression was suppressed by *PRR*s in wild-type background, but the PRR repression of *PIF4* was diminished in *elf3-1* mutant

background (Figure 11B). Similarly, the ELF3 function in repressing *PIF4* expression was also compromised in *prr5-1 toc1-21* mutant background (Figure 11B). Overall, these results demonstrate that PRRs and EC are interdependent and act together in the repression of *PIF4* and hypocotyl elongation.

3.7 Diurnal pattern of global H2A.Z deposition is mediated by PRRs-EC complex.

The EC has been demonstrated to interact with the SWR1 complex and establish repressive chromatin domains by catalyzing H2A.Z exchange, specifically during evening time (Tong et al., 2020). Thus, I sought to investigate whether the PRRs-EC complex also requires SWR1 to shape diurnal *PIF4* expression in a H2A.Z-dependent manner. To test this possibility, I analyzed H2A.Z distribution in genes targeted by PRRs and ELF3 (Table 1). H2A.Z signals in ELF3-target genes were increased at ZT16 compared to those at ZT4, and the night-specific increase in H2A.Z signals was compromised in *elf3-1* mutant (Figure 12), as previously demonstrated (Tong et al., 2020). In addition, although H2A.Z deposition of genes targeted solely by either PRR5 or TOC1 was comparable to randomly selected control genes, regardless of ZT points, H2A.Z distribution in genes commonly bound by PRR5 and TOC1 showed a significant increase in H2A.Z signal enrichment compared with that in control genes, specifically at ZT16 (Figure 12), suggesting that diurnal H2A.Z deposition is also regulated by PRRs, similar to ELF3. Furthermore, I also analyzed genes co-targeted by PRR5 (or TOC1) and EC and found that H2A.Z levels of co-target genes were additively elevated compared with those targeted by PRR5, TOC1, or ELF3 (Figure 12). Notably, the highest H2A.Z enrichment was shown in genes bound by all three PRR5, TOC1, and ELF3

proteins, and the synergistic H2A.Z enrichment was impaired in the *elf3-1* mutant (Figure 12), indicating that PRR5, TOC1, and EC synergistically enable H2A.Z deposition at co-target genes.

3.8 H2A.Z deposition at PIF4 locus is mediated by PRRs-EC-SWR1 complex.

To further corroborate the synergistic function of PRRs and EC in diurnal H2A.Z deposition at the *PIF4* locus, I examined H2A.Z enrichment in *elf3-1*, *prr5-1 toc1-21*, and *prr5-1 toc1-21 elf3-1* mutant. In wild type, the H2A.Z enrichment at the *PIF4* locus was significantly increased at nighttime relative to daytime (Figure 13). The night-specific H2A.Z deposition at the *PIF4* locus was reduced in *elf3-1* and *prr5-1 toc1-21* mutants (Figure 13 and 14A to 14D). Moreover, it was noteworthy that H2A.Z deposition at the *PIF4* locus is synergistically regulated by PRR5, TOC1, and EC, as the H2A.Z reduction was observed in broader region of *PIF4* in *prr5-1 toc1-21 elf3-1* mutant, compared with *elf3-1* and *prr5-1 toc1-21* mutants (Figure 14A to 14E).

The synergistic function among PRR5, TOC1, and the EC was related to the interaction with the SWR1 complex. Y2H assays showed that ELF3 interacted with SWR1 complex component SEF/SWC6 and the SANT domain of PIE1. PRR5 and TOC1 also interacted with the SANT domain of PIE1 (Figure 15A). Furthermore, I conducted Co-IP experiments using *Arabidopsis* protoplasts harboring 35S:*FLAG-PIE1*^{SANT}, *35S:HA-PRR5*, *35S:HA-TOC1* or *35S:MYC-ELF3* constructs. PRR5, TOC1, and ELF3 protein were co-immunoprecipitated when PIE1^{SANT} protein were pull down with anti-FLAG antibody (Figure 15B), indicating that PRR5, TOC1, and ELF3 interact with the SWR1 complex *in vivo*.

To quantify the interaction strength, I employed split luciferase analysis using *Arabidopsis* protoplasts. The ELF3-PIE1^{SANT} interaction was more strengthened by co-expressing PRR5 or TOC1 (Figure 15C). Moreover, simultaneous expression of the PRR5 and TOC1 further enhanced the interaction with the SWR1 complex, indicating that the PRR-EC-SWR1 complex formation underlies synergistic H2A.Z deposition as well as *PIF4* repression (Figure 15C).

The PRR-EC complex is likely dependent on H2A.Z deposition in repression of *PIF4* expression and hypocotyl elongation. The SWR1 complex participates in the control of circadian oscillation and hypocotyl growth (Kumar and Wigge, 2010; Mao et al., 2021; Tong et al., 2020; Wei et al., 2021; Xue et al., 2021). Consistently, hypocotyl lengths of *sef-1* and *arp6-1* mutants were longer than wild-type seedlings in my growth conditions (Figure 16A and 16B), as shown by *prr5-1*, *toc1-21*, and *elf3-1* mutants. Furthermore, *PIF4* expression in *arp6-1* mutant was significantly increased at ZT16 (Figure 16C), consistent with increased *PIF4* expression in *prr5-1*, *toc1-21*, and *elf3-1* mutants (Figure 7A). In addition, H2A.Z enrichment at *PIF4* gene body was substantially diminished in *arp6* and *pie1* mutants as observed in *elf3-1* mutant (Figure 16D). Overall, the PRRs and the EC simultaneously repress *PIF4* transcription through synergistic H2A.Z deposition in concert with SWR1 complex, which consequently shapes diurnal hypocotyl growth (Figure 17).

4. DISCUSSION

4.1 Synergistic functions of PRRs and EC in the repression of hypocotyl elongation.

The architecture of circadian clock is composed of multiple transcriptional negative feedback loops established by transcription factors, and cooperative actions of circadian oscillators associate to elaborately adjust the circadian clock and output pathways. In the morning, MYB transcription factor CIRCADIAN CLOCK ASSOCIATED 1 (CCA1) forms homodimers or heterodimers with LATE ELONGATED HYPOCOTYLS (LHY) to synergistically maintain circadian rhythm and induce *PIF4* expression (Sun et al., 2019; Yakir et al., 2009). Here, my findings elucidate the epigenetic mechanism underlying the formation of PRRs-EC-SWR1 complex at night. H2A.Z nucleosome catalyzing activity of SWR1 complex was synergistically regulated by PRR5, TOC1, and the EC, thereby repressing hypocotyl growth at nighttime.

Although how PRRs participate in epigenetic modification remained elusive, my data indicates that PRRs deposit H2A.Z nucleosome together with the SWR1 complex. Notably, H2A.Z deposition by PRR5 and TOC1 was synergistical with ELF3 in an ELF3-dependent manner. Intriguingly, growth inhibition by TOC1 under continuous light seems independent on ELF3 (Zhu et al., 2016), implying that hypocotyl regulation via H2A.Z deposition by PRRs-EC module takes place specifically under diurnal conditions. Considering diverse histone modifiers that interact with the EC to modulate various physiologies (Lee and Seo, 2021; Lee et al., 2019; Park et al., 2019), the possibility that other chromatin modifiers are recruited to the PRRs-EC module cannot be ruled out, thus further investigations

are required.

4.2 Broad role of H2A.Z in hypocotyl elongation.

The SWR1 complex gates hypocotyl elongation at multiple levels. The SWR1 complex subunits SEF/SWC6 and ARP6 physically interact with active Pfr form of phyB for inactivation of auxin biosynthesis genes *YUCCA9* (Wei et al., 2021). In addition to phyB, the SEF/SWC6 and ARP6 interacts with CRYPTOCHROME 1 (CRY1) in a blue light-dependent manner for recruitment of the SWR1 complex at *HY5* target locus (Mao et al., 2021). My study indicates that the SWR1 complex associates diurnal repressive chromatin domain at *PIF4* locus at night, thus broaden the understanding of SWR1 complex in hypocotyl elongation. Furthermore, considering the cooperation of the SWR1 complex with photoreceptors (phyB and CRY1) and circadian oscillators (PRRs and the EC), it is apparent that the SWR1 complex contributes to a broad spectrum of light-mediated growth regulation in plants.

Transcriptional regulation by H2A.Z nucleosomes are crucial in plant thermomorphogenesis. ARP6 regulate global H2A.Z deposition in response to external temperature changes (Kumar and Wigge, 2010). Recent study demonstrates that INO80 chromatin remodeling complex interacts with PIF4 protein to mediate H2A.Z eviction at PIF4 target loci at high temperature (Xue et al., 2021). The EC serves as a thermosensor in plant through temperature-dependent liquid-liquid phase separation (LLPS) (Ding et al., 2018; Jung et al., 2020; Thines and Harmon, 2010; Zhang et al., 2021). In addition, PRR5 and TOC1 also participate in thermomorphogenesis and form nuclear speckles (Hwang et al., 2021; Morris et al., 2019; Paffendorf et al., 2020; Strayer et al., 2000; Wang et al.,

2010; Zhu et al., 2016). Thus, the PRRs-EC-SWR1 complex may form circadian/temperature-dependent chromatin hotspots that integrate multiple signals from external environment into plant growth regulation.

5. FIGURES

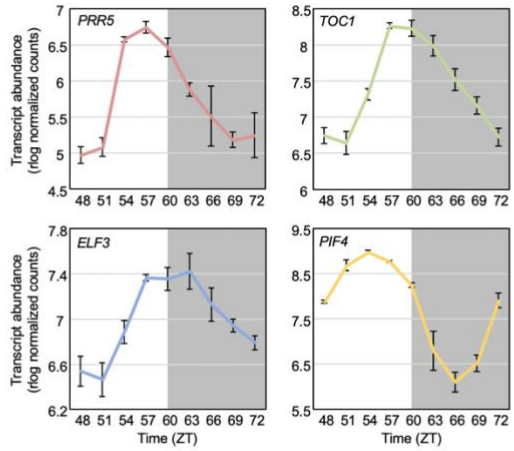

Figure 1. Circadian expression pattern of *PRR5*, *TOC1*, *ELF3*, and *PIF4*.

Transcript abundance *PRR5*, *TOC1*, *ELF3*, and *PIF4* during 24-h time course at 22 °C. Data from CAST-R were used to compare expression levels (Bonnot et al., 2022). The grey areas represent the subjective night. Error bars indicate ± SD.

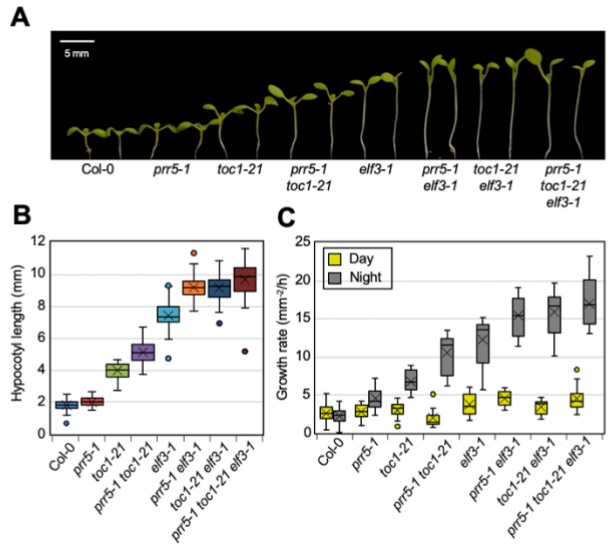

Figure 2. PRR5, TOC1, and ELF3 additively suppress hypocotyl growth at night.

(A) Representative image of 7-day-old Col-0, *prr5-1*, *toc1-21*, *prr5-1 toc1-21*, *efl3-1*, *prr5-1 elf3-1*, *toc1-21 elf3-1*, and *prr5-1 toc1-21 elf3-1* seedlings grown under 22 ℃ ND conditions. Scale bar = 5 μm. (B) Hypocotyl length measurements of circadian oscillator mutant seedlings. Seedlings were grown under 22 ℃ ND for 7 days. (C) Comparison between hypocotyl growth rate during day and night. Seedlings grown under 22 ℃ ND were imaged under infrared light. Yellow and gray color indicates averaged hypocotyl growth during day and night, respectively. In (B) and (C), boxes indicate boundaries of second and third quartiles of data distribution, and whiskers indicate the first and fourth quartiles. Black bars indicate the median value and cross marks indicate the mean value of data.

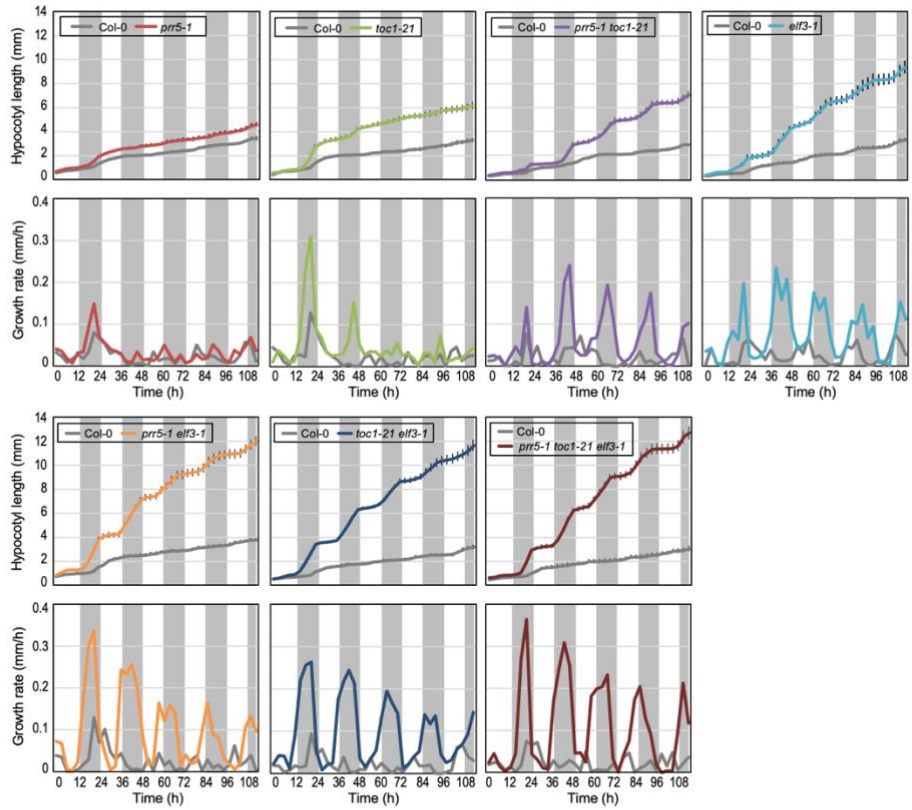

Figure 3. Dynamics of hypocotyl growth in circadian oscillator mutants.

Kinetics of hypocotyl elongation and growth rate in circadian oscillator mutants. Seedlings were imaged every 3 hours intervals for 5-days at 22°C ND conditions. Black bars represent ± SEM, n > 12.

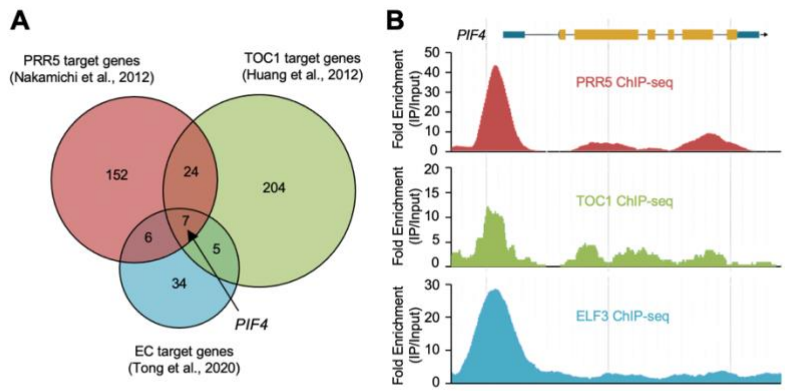

Figure 4. *PIF4* is co-regulated by PRR5, TOC1, and ELF3.

(A) A Venn diagram of genes targeted by PRR5, TOC1, and ELF3 within upstream 1kb from TSS of target genes. (B) Genome-browser view of ChIP-seq peaks at *PIF4* locus (AT2G43010).

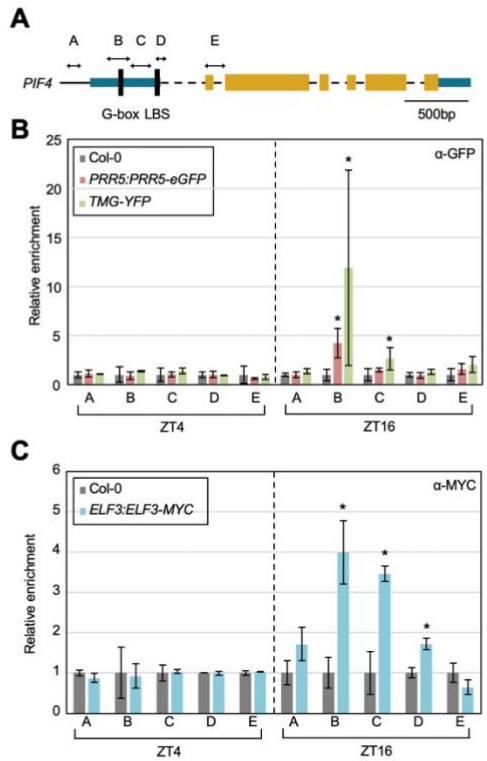

Figure 5. PRR5, TOC1, and ELF3 bind at *PIF4* locus at night.

(A) Genomic structure of *PIF4* gene. Turquoise boxes indicate 5' and 3' UTRs. Yellow boxes indicate exons. Arrows indicate the regions analyzed by quantitative PCR (qPCR) following chromatin immunoprecipitation (ChIP). Black lines indicate G-box and the LUX binding site (LBS). Binding of PRR5, and TOC1 (B), and ELF3 (C) at *PIF4* locus. Two-week-old seedlings entrained under ND cycles were harvested at ZT4 and ZT16 for ChIP-qPCR analysis. The enrichment of DNA was normalized to that of the *eIF4a* locus. Data represent mean ± SEM. (*$p < 0.05$; Student's t-test).

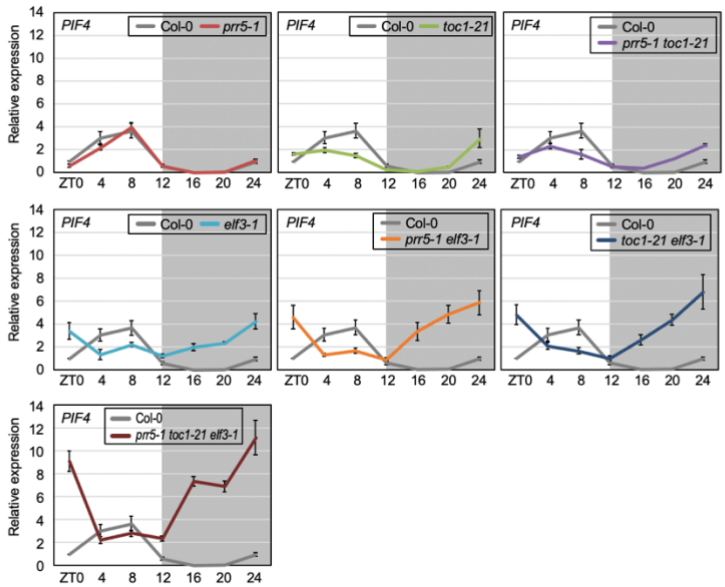

Figure 6. Diurnal *PIF4* expression in circadian oscillator mutants.

Time course expression of *PIF4*. Two-week-old seedlings were grown under 22°C ND conditions. Transcript levels were determined by RT-qPCR and values were normalized against *eIF4a* expression. Error bars indicate the standard error of the mean.

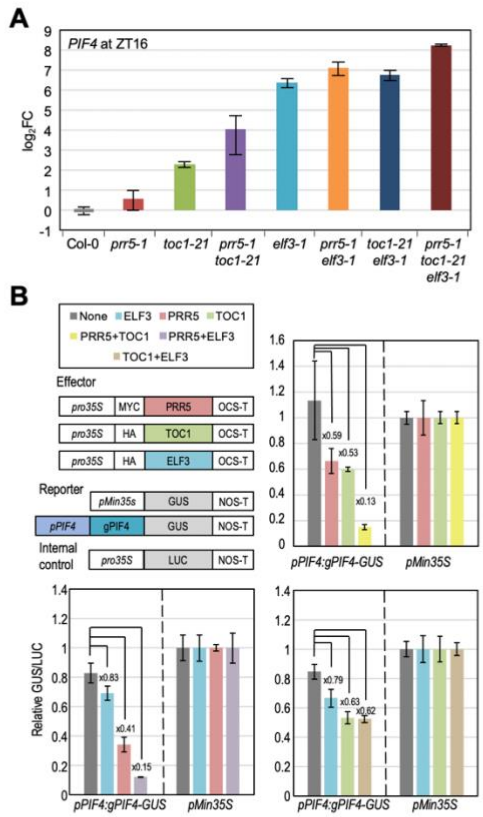

Figure 7. *PIF4* is synergistically repressed by PRR5, TOC1, and ELF3 at night.

(A) *PIF4* expression in Col-0, *prr5-1*, *toc1-21*, *prr5-1 toc1-21*, *efl3-1*, *prr5-1 elf3-1*, *toc1-21 elf3-1*, and *prr5-1 toc1-21 elf3-1* seedlings. 2-week-old seedlings grown under 22 °C ND were harvested at ZT16. Transcript levels were quantified by RT-qPCR. Gene expression values were normalized against *eIF4a* expression. The fold changes were calculated relative to the value of Col-0 seedlings and represented in $\log_2$FC. Error bars indicate ± SEM of biological triplicates. (B) Transient expression analysis using *Arabidopsis* mesophyll protoplasts. The effector constructs for PRR5, TOC1, and ELF3 expression and reporter constructs containing the promoter and genomic sequence of *PIF4* gene were transiently co-expressed in wild-type (Col-0) background. GUS activity was normalized to LUC

activity. Error bars indicate ± SEM of biological triplicates. Numbers indicate fold reduction by the effector constructs.

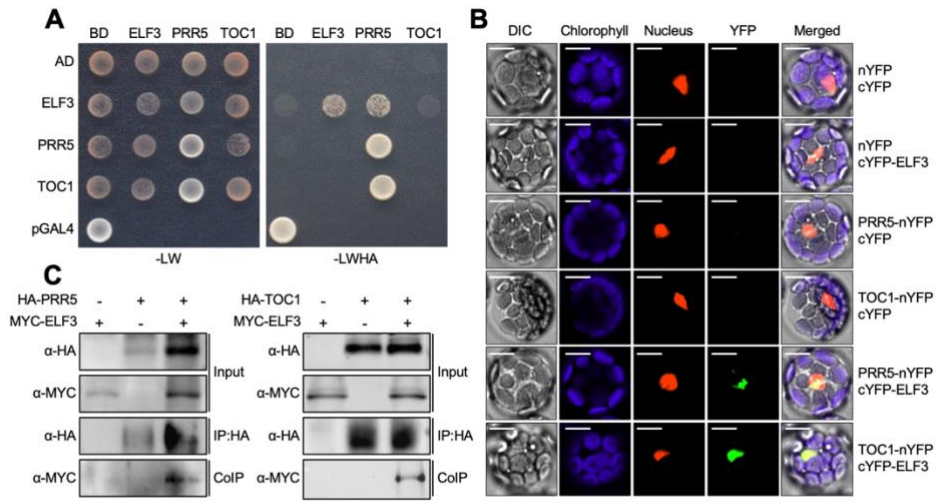

Figure 8. Formation of PRRs-EC complex.

(A) Y2H assays were performed with PRR5, TOC1, and ELF3 protein fused to either the DNA binding domain (BD) of GAL4 or the transcriptional activation domain (AD) of GAL4. Full-length GAL4 was used as a positive control. -LW indicates Leu and Trp dropout plates, and -LWHA indicates Leu, Trp, His and Ade dropout plates. (B) Bimolecular fluorescence complementation (BiFC) assays were conducted using *Arabidopsis* protoplasts. N-terminal or C-terminal fragments of YFP (nYFP or cYFP) fused to PRR5, TOC1, and ELF3 and the recombinant proteins were co-expressed along with nucleus marker (NLS-mCherry). Scale bars = 20μm. (C) Co-immunoprecipitation assays were performed with *Arabidopsis* protoplasts transiently expressing *35S:HA-PRR5*, *35S:HA-TOC1* and *35S:MYC-ELF3* constructs. Epitope-tagged proteins were immunoprecipitated with anto-HA magnetic beads and detected by western blotting using anti-HA and anti-MYC antibodies.

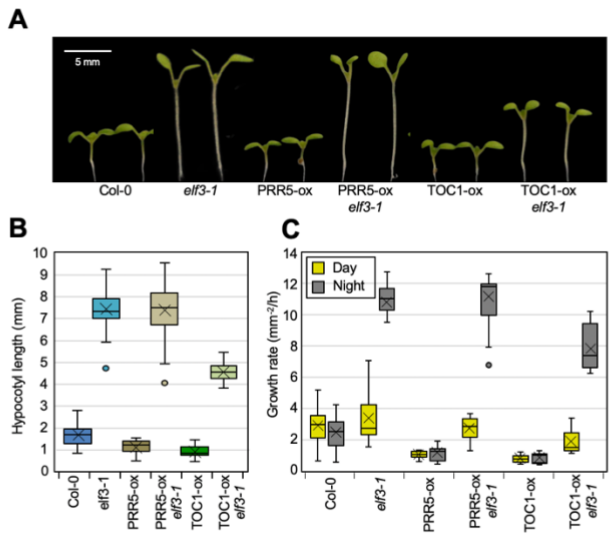

Figure 9. Repression of hypocotyl elongation by PRRs occurs in an ELF3-dependent manner.

(A) Representative image of 7-day-old Col-0, *elf3-1*, PRR5-ox, PRR5-ox/*elf3-1*, TOC1-ox, and TOC1-ox/*elf3-1* seedlings grown under 22 ℃ ND. Scale bar = 5 mm. (B) Hypocotyl length measurements of transgenic seedlings from (A). (C) Comparison between hypocotyl growth rate during day and night. Yellow and gray color indicates averaged hypocotyl growth during day and night, respectively. In (B) and (C), boxes indicate the boundaries of the second and third quartiles of data distribution, and whiskers indicate the first and fourth quartiles. Black bars indicate the median value and cross marks indicate the mean value of data.

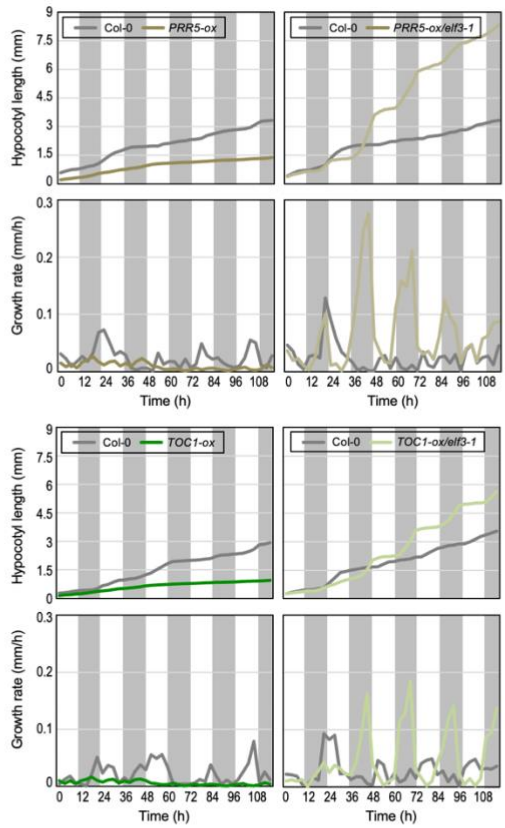

Figure 10. Dynamics of hypocotyl growth in *PRR5* and *TOC1* overexpressing plants.

Kinetics of hypocotyl elongation and growth rate in *PRR5* or *TOC1* overexpressing transgenic plants. Seedlings were imaged every 3 hours intervals for 5-days at 22°C ND conditions. Black bars represent ± SEM, n > 12.

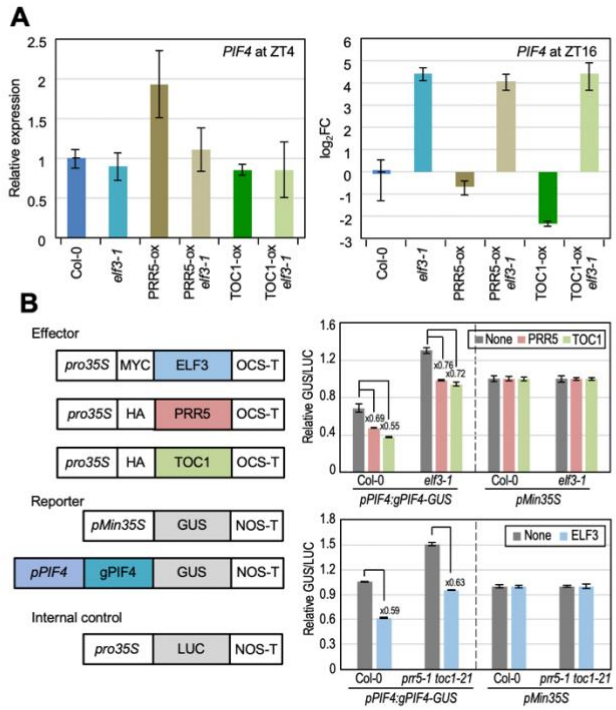

Figure 11. *PIF4* repression by PRRs and the EC is interdependent.

(A) *PIF4* expression in Col-0, PRR5-ox, PRR5-ox/*elf3-1*, TOC1-ox, and TOC1-ox/*elf3-1* seedlings. 2-week-old seedlings grown under 22 ℃ ND were harvested at ZT4 and ZT16. Transcript levels were quantified by RT-qPCR. Gene expression values were normalized against *eIF4a* expression. Relative gene expression values are represented as *n*-fold (left, ZT4) or $\log_2$FC (right, ZT16), relative to the value of wild-type (Col-0). Error bars indicate ± SEM of biological triplicates. (B) Transient expression analysis using *Arabidopsis* mesophyll protoplasts. The effector and reporter constructs were transiently co-expressed in wild-type (Col-0), *elf3-1*, and *prr5-1 toc1-21* background. GUS activity was normalized to LUC activity. Error bars indicate ± SEM of biological triplicates. Numbers indicate fold reduction by the effector constructs.

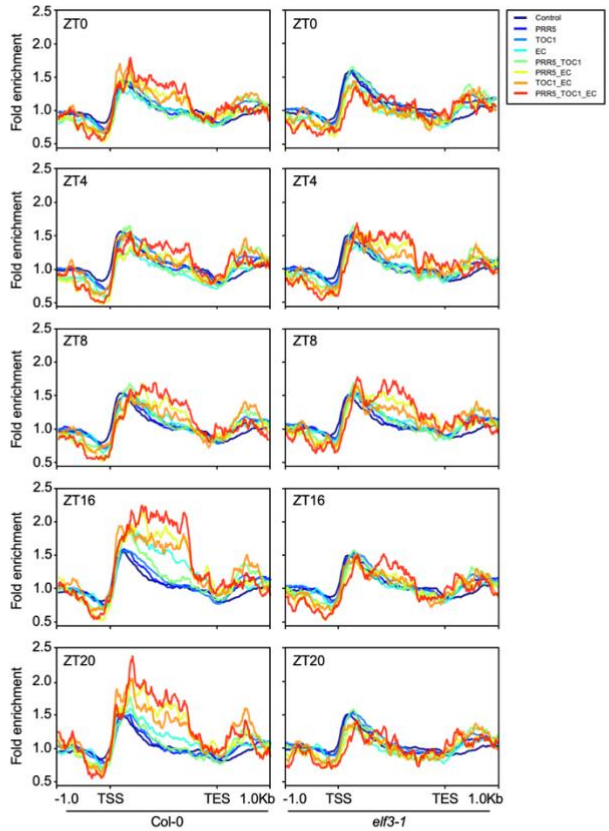

Figure 12. Diurnal H2A.Z deposition at PRR5, TOC1, and ELF3 target loci.

Diurnal H2A.Z occupancy of circadian components targeted genes in wild-type (Col-0), and *elf3-1* seedlings (See Table 1 for target gene list). H2A.Z ChIP-seq data were downloaded from a previous study (Tong et al., 2020). H2A.Z enrichment was represented as fold enrichment (IP/Input) of mapped reads. H2A.Z enrichment of randomly selected 240 genes was used as control. TSS, transcriptional start site; TES, transcription end site.

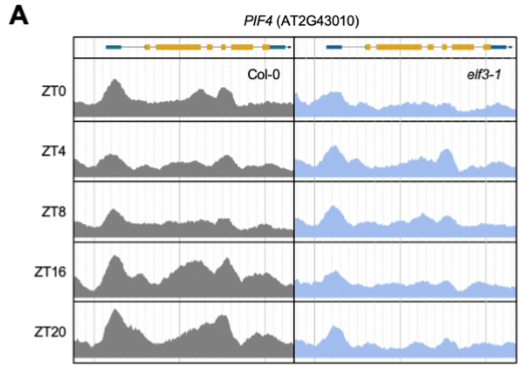

Figure 13. Diurnal H2A.Z deposition at *PIF4* locus in Col-0, and *elf3-1* mutant.

Diurnal H2A.Z occupancy at *PIF4* locus. H2A.Z enrichment was visualized using the genome browser provided by iRegNet (Shim et al., 2021).

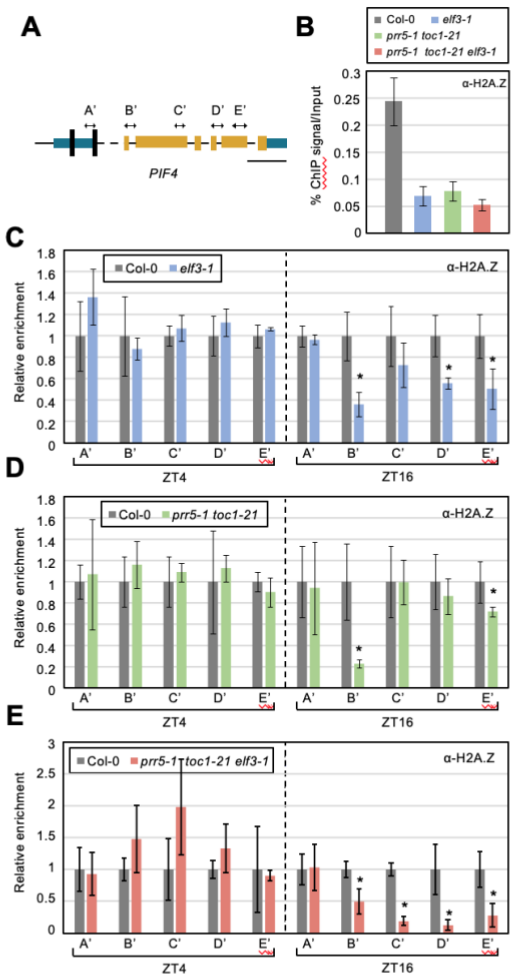

Figure 14. H2A.Z deposition is compromised in circadian oscillator mutants.

(A) Genomic structure of *PIF4* gene. Arrows indicate the regions analyzed by quantitative PCR (qPCR) following chromatin immunoprecipitation (ChIP). Black lines indicate G-box and the LUX binding site (LBS). (B) H2A.Z levels at the B' locus of *PIF4* in Col-0, *elf3-1*, *prr5-1 toc1-21*, and *prr5-1 toc1-21 elf3-1* mutants at ZT16. H2A.Z deposition at *PIF4* locus at ZT4 and ZT16 in (C) *elf3-1*, (D) *prr5-1 toc1-21*, and (E) *prr5-1 toc1-21 elf3-1* seedlings. For (C) to (E), two-week-old seedlings entrained under ND cycles were harvested at ZT4 and ZT16. The enrichment of precipitated DNA was analyzed by ChIP-qPCR and normalized to

that of the *eIF4a* locus. Error bars indicate ± SEM of biological triplicates. (*p < 0.05; Student's t-test).

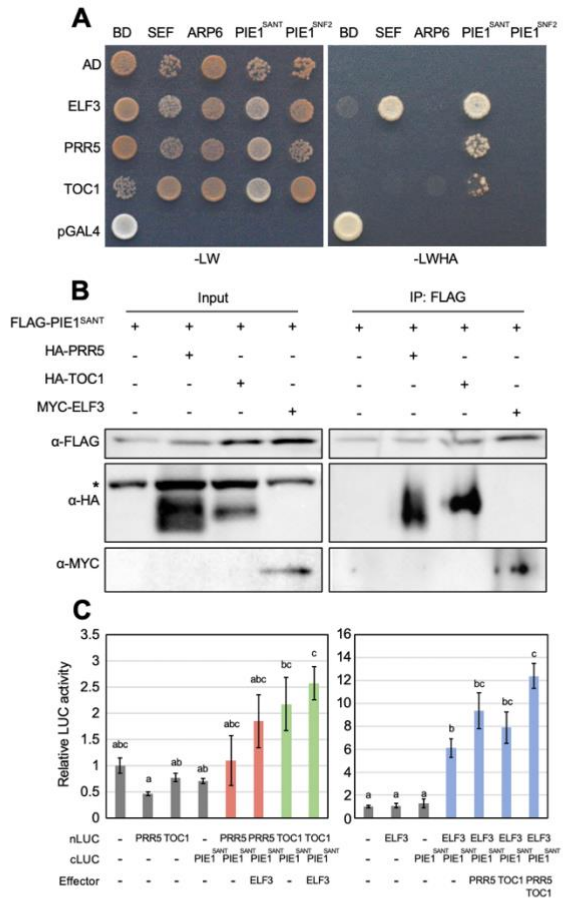

Figure 15. Formation of the PRRs-EC-SWR1 complex.

(A) Y2H assays were performed with PRR5, TOC1, and ELF3 protein fused to the transcriptional activation domain (AD) of GAL4, and SWR1 complex components SEF, ARP6, PIE1^{SANT}, and PIE1^{SNF2} protein fused to the DNA binding domain (BD) of GAL4. Full-length GAL4 was used as a positive control. -LW indicates Leu and Trp dropout plates, and -LWHA indicates Leu, Trp, His and Ade dropout plates. (B) Co-immunoprecipitation assays were performed with *Arabidopsis* protoplasts transiently expressing 35S:FLAG-PIE1^{SANT}, 35S:HA-PRR5, 35S:HA-TOC1 and 35S:MYC-ELF3 constructs. Epitope-tagged proteins were immunoprecipitated with anti-FLAG magnetic beads and detected by western

blotting. (C) Split luciferase assays were performed with the N-terminal fragment of luciferase fused to C-terminal of PRR5, TOC1, and ELF3 protein, while the C-terminal fragment of luciferase fused to N-terminal of $PIE1^{SANT}$ protein. PRR5, TOC1, or ELF3 overexpressing effector plasmids and GUS overexpressing internal control plasmids were co-transfected. LUC activity was normalized to GUS activity. Error bars indicate ± SEM of biological triplicates. The letters above the bars indicate the significant differences determined by one-way ANOVA.

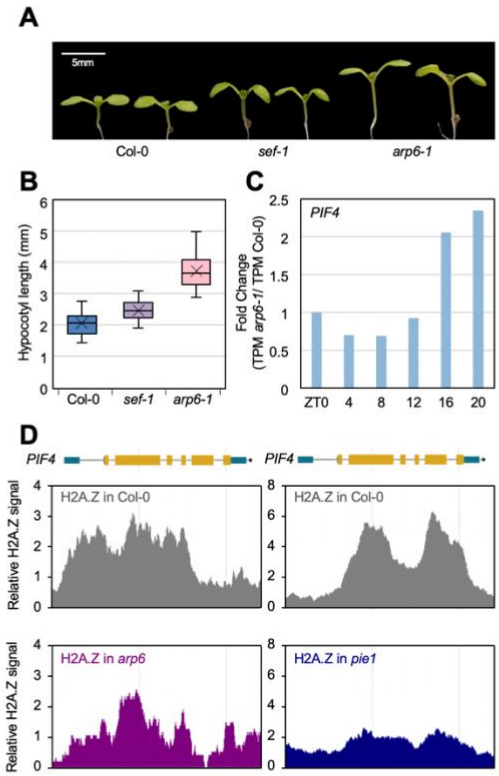

Figure 16. The SWR1 complex mediates H2A.Z deposition at *PIF4* locus for hypocotyl growth regulation.

(A) Representative image of 7-day-old Col-0, *sef-1*, and *arp6-1* seedlings grown under 22 ℃ ND. Scale bar = 5 mm. (B) Hypocotyl length measurements of transgenic seedlings from (A). Boxes indicate boundaries of second and third quartiles of data distribution, and whiskers indicate the first and fourth quartiles. Black bars indicate median value and cross marks indicate mean value of data. (C) Diurnal *PIF4* expression in *arp6-1* mutant. RNA-seq data were acquired from previous study (Tong et al., 2020). (D) Relative H2A.Z signals in *arp6* and *pie1* mutants were visualized using the genome browser provided by iRegNet (Shim et al., 2021).

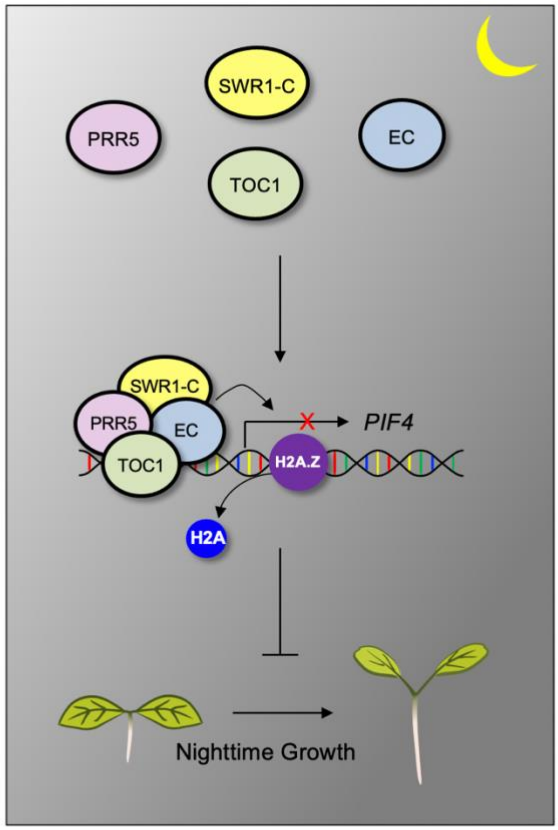

Figure 17. Nighttime hypocotyl growth repression mediated by H2A.Z deposition by PRRs-EC-SWR1 complex at *PIF4* locus.

At dusk, PRR5, TOC, the EC, and the SWR1 complex assemble into a protein complex, which deposits H2A.Z nucleosomes at *PIF4* region. Thus, *PIF4* expression is repressed, consequently impedes hypocotyl growth during nighttime.

6. TABLES

PRR5, TOC1, EC co-targeted genes (7)

AGI number	Gene Name
AT1G02350	-
AT2G43010	PHYTOCHROME INTERACTING FACTOR 4 (PIF4)
AT2G46790	PSEUDO-RESPONSE REGULATOR 9 (PRR9)
AT3G12320	NIGHT LIGHT-INDUCIBLE AND CLOCK-REGULATED GENE 3 (LNK3)
AT3G46640	LUX ARRHYTHMO (LUX)
AT4G27310	B-BOX DOMAIN PROTEIN 28 (BBX28)
AT5G02580	-

PRR5, TOC1 co-targeted genes (31)

AGI number	Gene Name
AT1G02350	-
AT1G02065	SQUAMOSA PROMOTER BINDING PROTEIN-LIKE 8 (SPL8)
AT1G02350	-
AT1G09350	GALACTINOL SYNTHASE 3 (GolS3)
AT1G18740	BYPASS1-LIKE (B1L)
AT1G68020	TREHALOSE-6-PHOSPHATASE SYNTHASE S6 (TPS6)
AT1G73670	MAP KINASE 15 (MPK15)
AT1G74450	ROH1D
AT2G18790	PHYTOCHROME B (PHYB)
AT2G20580	26S PROTEASOME REGULATORY SUBUNIT S2 1A (RPN1A)
AT2G28130	ARABIDOPSIS SNI1 ASSOCIATED PROTEIN 1 (ASAP1)
AT2G31380	B-BOX DOMAIN PROTEIN 25 (BBX25)
AT2G33510	CFL1

AT2G43010	PHYTOCHROME INTERACTING FACTOR 4 (PIF4)
AT2G46790	PSEUDO-RESPONSE REGULATOR 9 (PRR9)
AT2G46830	CIRCADIAN CLOCK ASSOCIATED 1 (CCA1)
AT3G12320	NIGHT LIGHT-INDUCIBLE AND CLOCK-REGULATED GENE 3 (LNK3)
AT3G19590	BUDDING UNINHIBITED BY BENZYMIDAZOL 3.1 (BUB3.1)
AT3G46640	LUX ARRHYTHMO (LUX)
AT3G60400	SUPPRESSOR OF HOT1-4 1 (SHOT1)
AT3G61630	CYTOKININ RESPONSE FACTOR 6 (CRF6)
AT4G18890	BES1/BZR1 HOMOLOG 3 (BEH3)
AT4G21930	-
AT4G27310	B-BOX DOMAIN PROTEIN 28 (BBX28)
AT5G02200	FAR-RED-ELONGATED HYPOCOTYL1-LIKE (FHL)
AT5G02580	-
AT5G02820	BRASSINOSTEROID INSENSITIVE 5 (BIN5)
AT5G13100	-
AT5G13640	PHOSPHOLIPID:DIACYLGLYCEROL ACYLTRANSFERASE 1 (PDAT1)
AT5G41600	RETICULAN LIKE PROTEIN B4 (RTNLB4)
AT5G51460	TREHALOSE-6-PHOSPHATE PHOSPHATASE A (TPPA)

PRR5, EC co-targeted genes (13)

AGI number	Gene Name
AT1G02350	-
AT1G22770	SQUAMOSA PROMOTER BINDING PROTEIN-LIKE 8 (SPL8)
AT1G73480	MAGL4
AT2G43010	PHYTOCHROME-INTERACTING FACTOR 4 (PIF4)
AT2G46790	PSEUDO-RESPONSE REGULATOR 9 (PRR9)

AT3G12320	NIGHT LIGHT-INDUCIBLE AND CLOCK-REGULATED GENE 3 (LNK3)
AT3G46640	LUX ARRHYTHMO (LUX)
AT4G27310	B-BOX DOMAIN PROTEIN 28 (BBX28)
AT4G36040	DNA J PROTEIN C23 (DJC23);DNAJ11 (J11)
AT5G02580	-
AT5G06980	NIGHT LIGHT-INDUCIBLE AND CLOCK-REGULATED GENE 4 (LNK4)
AT5G39860	BANQUO 1 (BNQ1)
AT5G64180	-

TOC1, EC co-targeted genes (12)

AGI number	Gene Name
AT1G02350	-
AT1G75450	CYTOKININ OXIDASE 5 (CKX5)
AT2G40340	DREB2C
AT2G43010	PHYTOCHROME-INTERACTING FACTOR 4 (PIF4)
AT2G46790	PSEUDO-RESPONSE REGULATOR 9 (PRR9)
AT3G12320	NIGHT LIGHT-INDUCIBLE AND CLOCK-REGULATED GENE 3 (LNK3)
AT3G46640	LUX ARRHYTHMO (LUX)
AT3G53830	-
AT3G59060	PHYTOCHROME-INTERACTING FACTOR 5 (PIF5)
AT4G27310	B-BOX DOMAIN PROTEIN 28 (BBX28)
AT5G02580	-
AT5G02810	PSEUDO-RESPONSE REGULATOR 7 (PRR7)

Table 1. List of genes co-targeted by PRR5, TOC1, and EC

Primer	Usage	Sequence
eIF4a-F	RT-qPCR	5′-TGACCACACAGTCTCTGCAA
eIF4a-R	RT-qPCR	5′-ACCAGGGAGACTTGTTGGAC
PIF4-F	RT-qPCR	5′-AGATCATCTCCGACCGGTTT
PIF4-R	RT-qPCR	5′-CGCCGGTGAACTAAATCTCA
PIF4(A)-F	ChIP-qPCR	5′-GCCAAGGGTGCCCTTTCAATGC
PIF4(A)-R	ChIP-qPCR	5′-CCGAGTTCAATGCTCTCAACGAGT
PIF4(B)-F	ChIP-qPCR	5′-CTAAAAATCAAGCAATAGATCTC
PIF4(B)-R	ChIP-qPCR	5′-ACAGGAGCATAAAGATATTACAG
PIF4(C)-F	ChIP-qPCR	5′-TGCTCCTGTCACTTTCTGTCTGTACCC
PIF4(C)-R	ChIP-qPCR	5′-TCCAAGTTCCACGCCCAACACA
PIF4(D)-F	ChIP-qPCR	5′-TCTGATTCGTCCAGAAGCTTTCCT
PIF4(D)-R	ChIP-qPCR	5′-GCCACATCTTATAAAACCAAAAACCCG
PIF4(E)-F	ChIP-qPCR	5′-ACACCAAGGTTGGAGTTTTGAGGA
PIF4(E)-R	ChIP-qPCR	5′-TGGCCTAGACATCAATACACACACACACA
PIF4(A′)-F	ChIP-qPCR	5′-gtgagttgtttctcaacaattttc
PIF4(A′)-R	ChIP-qPCR	5′-cttctggacgaatcagaagttg
PIF4(B′)-F	ChIP-qPCR	5′-ACACCAAGGTTGGAGTTTTGAGGA
PIF4(B′)-R	ChIP-qPCR	5′-TGGCCTAGACATCAATACACACACACACA
PIF4(C′)-F	ChIP-qPCR	5′-AAGCAAAAACATAGAAGAAAAG
PIF4(C′)-R	ChIP-qPCR	5′-TTTATACGTTTTCTCTTACGGTC
PIF4(D′)-F	ChIP-qPCR	5′-GAGGAGGAGAGATAGGATCAATG
PIF4(D′)-R	ChIP-qPCR	5′-CGAAGCTTTATCAGTCTGCAAA
PIF4(E′)-F	ChIP-qPCR	5′-TCCCCGGAGTTCAACCTCAGCA
PIF4(E′)-R	ChIP-qPCR	5′-GAGTCGCGGCCTGCATGTGT
PRR5-F	Cloning	5′-CCCATACGATGTTCCAGATTACGCTATGACTAGTAGC GAGGAAGTAGTTG
PRR5-R	Cloning	5′-ATTAACTCTCTAGACTCACCTAGGCCTATGGAGCTTG TGTGGATTGG
TOC1-F	Cloning	5′-CCCATACGATGTTCCAGATTACGCTATGGATTTGAAC GGTGAGTGTAAAG
TOC1-R	Cloning	5′-ATTAACTCTCTAGACTCACCTAGGCTCAAGTTCCCAA AGCATCATCC
ELF3-F	Cloning	5′-GATCTCTGAAGAAGATCTGATCgggATGAAGAGAGGG AAAGATGAGGA
ELF3-R	Cloning	5′-TAGACTCACCTAGATTAACTCTCggTTAAGGCTTAGA GGAGTCATAGCG
PIE1-F	Cloning	5′-CAAAGACGATGACGACAAAATCgggGCTCAGCACCAG TTAATGGAAG
PIE1-R	Cloning	5′-TAGACTCACCTAGATTAACTCTCggTCATGCTAAGAG TTTGCGGTGTTT
pPIF4-F	Cloning	5′-tcacacaggaaacagctatgACATGgggtctcgtttc gtacaacaaag
pPIF4-R	Cloning	5′-gtcagatctctggagacatttca
gPIF4-F	Cloning	5′-tgaaatgtctccagagatctgac
gPIF4-R	Cloning	5′-ttccttatatagaggaagggtcttaccGTGGTCCAAA CGAGAACCG

Table 2. List of primers used in this study

7. REFERENCES

Aslam, M., Fakher, B., Jakada, B.H., Cao, S., and Qin, Y. (2019). SWR1 chromatin remodeling complex: A key transcriptional regulator in plants. Cells *8*, 1621.

Bonnot, T., Gillard, M.B., and Nagel, D.H. (2022). CAST-R: An application to visualize circadian and heat stress–responsive genes in plants. Plant Physiology, kiac121.

Bonnot, T., and Nagel, D.H. (2021). Time of the day prioritizes the pool of translating mRNAs in response to heat stress. The Plant Cell *33*, 2164-2182.

Box, Mathew S., Huang, B.E., Domijan, M., Jaeger, Katja E., Khattak, Asif K., Yoo, Seong J., Sedivy, Emma L., Jones, D.M., Hearn, Timothy J., Webb, Alex A.R., *et al.* (2015). ELF3 controls thermoresponsive growth in Arabidopsis. Current Biology *25*, 194-199.

Coleman-Derr, D., and Zilberman, D. (2012). Deposition of histone variant H2A.Z within gene bodies regulates responsive genes. PLoS Genetics *8*, e1002988.

Covington, M.F., and Harmer, S.L. (2007). The circadian clock regulates auxin signaling and responses in Arabidopsis. PLOS Biology *5*, e222.

Deal, R.B., Kandasamy, M.K., McKinney, E.C., and Meagher, R.B. (2005). The nuclear actin-related protein ARP6 ss a pleiotropic developmental regulator required for the maintenance of FLOWERING LOCUS C expression and repression of flowering in Arabidopsis. The Plant Cell *17*, 2633-2646.

Ding, L., Wang, S., Song, Z.-T., Jiang, Y., Han, J.-J., Lu, S.-J., Li, L., and Liu, J.-X. (2018). Two B-Box domain proteins, BBX18 and BBX23, interact with ELF3 and regulate thermomorphogenesis in Arabidopsis. Cell Reports *25*, 1718-1728.e1714.

Ding, Z., Doyle, M.R., Amasino, R.M., and Davis, S.J. (2007). A complex genetic

interaction between Arabidopsis thaliana TOC1 and CCA1/LHY in driving the circadian clock and in output regulation. Genetics *176*, 1501-1510.

Doyle, M.R., Davis, S.J., Bastow, R.M., McWatters, H.G., Kozma-Bognár, L., Nagy, F., Millar, A.J., and Amasino, R.M. (2002). The ELF4 gene controls circadian rhythms and flowering time in Arabidopsis thaliana. Nature *419*, 74.

Ezer, D., Jung, J.-H., Lan, H., Biswas, S., Gregoire, L., Box, M.S., Charoensawan, V., Cortijo, S., Lai, X., Stöckle, D., *et al.* (2017). The evening complex coordinates environmental and endogenous signals in Arabidopsis. Nature Plants *3*, 17087.

Gendron, J.M., Pruneda-Paz, J.L., Doherty, C.J., Gross, A.M., Kang, S.E., and Kay, S.A. (2012). Arabidopsis circadian clock protein, TOC1, is a DNA-binding transcription factor. Proceedings of the National Academy of Sciences *109*, 3167-3172.

Gibson, D.G., Young, L., Chuang, R.-Y., Venter, J.C., Hutchison, C.A., and Smith, H.O. (2009). Enzymatic assembly of DNA molecules up to several hundred kilobases. Nature Methods *6*, 343-345.

Gray William, M., Östin, A., Sandberg, G., Romano Charles, P., and Estelle, M. (1998). High temperature promotes auxin-mediated hypocotyl elongation in Arabidopsis. Proceedings of the National Academy of Sciences *95*, 7197-7202.

Hazen, S.P., Schultz, T.F., Pruneda-Paz, J.L., Borevitz, J.O., Ecker, J.R., and Kay, S.A. (2005). LUX ARRHYTHMO encodes a Myb domain protein essential for circadian rhythms. Proceedings of the National Academy of Sciences *102*, 10387-10392.

Helfer, A., Nusinow, D.A., Chow, B.Y., Gehrke, A.R., Bulyk, M.L., and Kay, S.A. (2011). LUX ARRHYTHMO encodes a nighttime repressor of circadian gene expression in the Arabidopsis core clock. Current Biology *21*, 126-133.

Hicks, K.A., Albertson, T.M., and Wagner, D.R. (2001). EARLY FLOWERING3 encodes a novel protein that regulates circadian clock function and flowering in Arabidopsis. The Plant Cell *13*, 1281-1292.

Huang, W., Perez-Garcia, P., Pokhilko, A., Millar, A.J., Antoshechkin, I., Riechmann, J.L., and Mas, P. (2012). Mapping the core of the Arabidopsis circadian clock defines the network structure of the oscillator. Science *336*, 75-79.

Huq, E., and Quail, P.H. (2002). PIF4, a phytochrome-interacting bHLH factor, functions as a negative regulator of phytochrome B signaling in *Arabidopsis*. The EMBO Journal *21*, 2441-2450.

Hwang, G., Park, J., Kim, S., Park, J., Seo, D., and Oh, E. (2021). Overexpression of BBX18 promotes thermomorphogenesis through the PRR5-PIF4 pathway. Frontiers in Plant Science *12*, 782352.

Jung, J.H., Barbosa, A.D., Hutin, S., Kumita, J.R., Gao, M., Derwort, D., Silva, C.S., Lai, X., Pierre, E., Geng, F., *et al.* (2020). A prion-like domain in ELF3 functions as a thermosensor in Arabidopsis. Nature *585*, 256-260.

Kaczorowski, K.A., and Quail, P.H. (2003). Arabidopsis PSEUDO-RESPONSE REGULATOR7 is a signaling intermediate in phytochrome-regulated seedling deetiolation and phasing of the circadian clock. The Plant Cell *15*, 2654-2665.

Klose, C., Venezia, F., Hussong, A., Kircher, S., Schäfer, E., and Fleck, C. (2015). Systematic analysis of how phytochrome B dimerization determines its specificity. Nature Plants *1*, 15090.

Koini, M.A., Alvey, L., Allen, T., Tilley, C.A., Harberd, N.P., Whitelam, G.C., and Franklin, K.A. (2009). High temperature-mediated adaptations in plant architecture require the bHLH transcription factor PIF4. Current Biology *19*, 408-413.

Kumar, S.V. (2018). H2A.Z at the core of transcriptional regulation in plants.

Molecular Plant *11*, 1112-1114.

Kumar, S.V., and Wigge, P.A. (2010). H2A.Z-containing nucleosomes mediate the thermosensory response in Arabidopsis. Cell *140*, 136-147.

Langmead, B., and Salzberg, S.L. (2012). Fast gapped-read alignment with Bowtie 2. Nature Methods *9*, 357-359.

Lee, H.G., and Seo, P.J. (2021). The Arabidopsis JMJ29 protein controls circadian oscillation through diurnal histone demethylation at the CCA1 and PRR9 loci. Genes *12*, 529.

Lee, K., Mas, P., and Seo, P.J. (2019). The EC-HDA9 complex rhythmically regulates histone acetylation at the TOC1 promoter in Arabidopsis. Communications Biology *2*, 143.

Lei, B., and Berger, F. (2020). H2A variants in Arabidopsis: Versatile regulators of genome activity. Plant Communications *1*, 100015.

Li, N., Zhang, Y., He, Y., Wang, Y., and Wang, L. (2020). Pseudo Response Regulators regulate photoperiodic hypocotyl growth by repressing PIF4/5 transcription. Plant Physiol *183*, 686-699.

Liu, T., Carlsson, J., Takeuchi, T., Newton, L., and Farre, E.M. (2013). Direct regulation of abiotic responses by the Arabidopsis circadian clock component PRR7. Plant Journal *76*, 101-114.

Liu, X.L., Covington, M.F., Fankhauser, C., Chory, J., and Wagner, D.R. (2001). ELF3 encodes a circadian clock–regulated nuclear protein that functions in an Arabidopsis PHYB signal transduction pathway. The Plant Cell *13*, 1293-1304.

Lorrain, S., Allen, T., Duek, P.D., Whitelam, G.C., and Fankhauser, C. (2008). Phytochrome-mediated inhibition of shade avoidance involves degradation of growth-promoting bHLH transcription factors. The Plant Journal *53*, 312-323.

Lu, S.X., Webb, C.J., Knowles, S.M., Kim, S.H.J., Wang, Z., and Tobin, E.M. (2012). CCA1 and ELF3 interact in the control of hypocotyl length and flowering time in Arabidopsis. Plant Physiology *158*, 1079-1088.

Mao, Z., Wei, X., Li, L., Xu, P., Zhang, J., Wang, W., Guo, T., Kou, S., Wang, W., Miao, L., *et al.* (2021). Arabidopsis cryptochrome 1 controls photomorphogenesis through regulation of H2A.Z deposition. The Plant Cell *33*, 1961-1979.

March-DíAz, R., GarcíA-DomíNguez, M., Florencio, F.J., and Reyes, J.C. (2007). SEF, a new protein required for flowering repression in Arabidopsis, interacts with PIE1 and ARP6. Plant Physiology *143*, 893-901.

March-Díaz, R., and Reyes, J.C. (2009). The beauty of being a variant: H2A.Z and the SWR1 complex in plants. Molecular Plant *2*, 565-577.

Martín, G., Rovira, A., Veciana, N., Soy, J., Toledo-Ortiz, G., Gommers, C.M.M., Boix, M., Henriques, R., Minguet, E.G., Alabadí, D., *et al.* (2018). Circadian waves of transcriptional repression shape PIF-regulated photoperiod-responsive growth in Arabidopsis. Current Biology *28*, 311-318.e315.

Martínez, C., Espinosa-Ruíz, A., Lucas, M., Bernardo-García, S., Franco-Zorrilla, J.M., and Prat, S. (2018). PIF4-induced BR synthesis is critical to diurnal and thermomorphogenic growth. The EMBO Journal *37*, e99552.

Más, P., Alabadí, D., Yanovsky, M.J., Oyama, T., and Kay, S.A. (2003). Dual role of TOC1 in the control of circadian and photomorphogenic responses in Arabidopsis. The Plant Cell *15*, 223-236.

Morris, W.L., Ducreux, L.J.M., Morris, J., Campbell, R., Usman, M., Hedley, P.E., Prat, S., and Taylor, M.A. (2019). Identification of TIMING OF CAB EXPRESSION 1 as a temperature-sensitive negative regulator of tuberization in potato. Journal of Experimental Botany *70*, 5703-5714.

Murcia, G., Nieto, C., Sellaro, R., Prat, S., and Casal, J.J. (2022). Hysteresis in PHYTOCHROME-INTERACTING FACTOR 4 and EARLY-FLOWERING 3 dynamics dominates warm daytime memory in Arabidopsis. The Plant Cell, koac078.

Nakamichi, N., Kiba, T., Kamioka, M., Suzuki, T., Yamashino, T., Higashiyama, T., Sakakibara, H., and Mizuno, T. (2012). Transcriptional repressor PRR5 directly regulates clock-output pathways. Proceedings of the National Academy of Sciences *109*, 17123-17128.

Nieto, C., López-Salmerón, V., Davière, J.-M., and Prat, S. (2015). ELF3-PIF4 interaction regulates plant growth independently of the evening complex. Current Biology *25*, 187-193.

Niwa, Y., Yamashino, T., and Mizuno, T. (2009). The circadian clock regulates the photoperiodic response of hypocotyl elongation through a coincidence mechanism in Arabidopsis thaliana. Plant and Cell Physiology *50*, 838-854.

Nohales, M.A., Liu, W., Duffy, T., Nozue, K., Sawa, M., Pruneda-Paz, J.L., Maloof, J.N., Jacobsen, S.E., and Kay, S.A. (2019). Multi-level modulation of light signaling by GIGANTEA regulates both the output and pace of the circadian clock. Developmental cell *49*, 840-851 e848.

Nomoto, Y., Kubozono, S., Yamashino, T., Nakamichi, N., and Mizuno, T. (2012). Circadian clock- and PIF4-controlled plant growth: A coincidence mechanism directly integrates a hormone signaling network into the photoperiodic control of plant architectures in Arabidopsis thaliana. Plant and Cell Physiology *53*, 1950-1964.

Nusinow, D.A., Helfer, A., Hamilton, E.E., King, J.J., Imaizumi, T., Schultz, T.F., Farré, E.M., and Kay, S.A. (2011). The ELF4–ELF3–LUX complex links the

circadian clock to diurnal control of hypocotyl growth. Nature *475*, 398.

Oh, E., Zhu, J.-Y., and Wang, Z.-Y. (2012). Interaction between BZR1 and PIF4 integrates brassinosteroid and environmental responses. Nature Cell Biology *14*, 802-809.

Onai, K., and Ishiura, M. (2005). PHYTOCLOCK 1 encoding a novel GARP protein essential for the Arabidopsis circadian clock. Genes to Cells *10*, 963-972.

Paffendorf, B.A.M., Qassrawi, R., Meys, A.M., Trimborn, L., and Schrader, A. (2020). TRANSPARENT TESTA GLABRA 1 participates in flowering time regulation in Arabidopsis thaliana. PeerJ *8*, e8303.

Park, H.J., Baek, D., Cha, J.-Y., Liao, X., Kang, S.-H., McClung, C.R., Lee, S.Y., Yun, D.-J., and Kim, W.-Y. (2019). HOS15 interacts with the histone deacetylase HDA9 and the evening complex to epigenetically regulate the floral activator GIGANTEA. The Plant Cell *31*, 37-51.

Ramírez, F., Ryan, D.P., Grüning, B., Bhardwaj, V., Kilpert, F., Richter, A.S., Heyne, S., Dündar, F., and Manke, T. (2016). deepTools2: a next generation web server for deep-sequencing data analysis. Nucleic Acids Research *44*, W160-W165.

Sato, E., Nakamichi, N., Yamashino, T., and Mizuno, T. (2002). Aberrant expression of the Arabidopsis circadian-regulated APRR5 gene belonging to the APRR1/TOC1 quintet results in early flowering and hypersensitiveness to light in early photomorphogenesis. Plant and Cell Physiology *43*, 1374-1385.

Seo, P.J., and Mas, P. (2015). STRESSing the role of the plant circadian clock. Trends in Plant Science *20*, 230-237.

Shim, S., Park, C.-M., and Seo, P.J. (2021). iRegNet: an integrative Regulatory Network analysis tool for Arabidopsis thaliana. Plant Physiology *187*, 1292-1309.

Silva, C.S., Nayak, A., Lai, X., Hutin, S., Hugouvieux, V., Jung, J.-H., López-

Vidriero, I., Franco-Zorrilla, J.M., Panigrahi, K.C.S., Nanao, M.H., *et al.* (2020). Molecular mechanisms of Evening Complex activity in Arabidopsis. Proceedings of the National Academy of Sciences *117*, 6901-6909.

Soy, J., Leivar, P., González-Schain, N., Martín, G., Diaz, C., Sentandreu, M., Al-Sady, B., Quail, P.H., and Monte, E. (2016). Molecular convergence of clock and photosensory pathways through PIF3–TOC1 interaction and co-occupancy of target promoters. Proceedings of the National Academy of Sciences *113*, 4870-4875.

Steed, G., Ramirez, D.C., Hannah, M.A., and Webb, A.A.R. (2021). Chronoculture, harnessing the circadian clock to improve crop yield and sustainability. Science *372*, eabc9141.

Strayer, C., Oyama, T., Schultz, T.F., Raman, R., Somers, D.E., Mas, P., Panda, S., Kreps, J.A., and Kay, S.A. (2000). Cloning of the Arabidopsis clock gene TOC1, an autoregulatory response regulator homolog. Science *289*, 768-771.

Sun, J., Qi, L., Li, Y., Chu, J., and Li, C. (2012). PIF4–mediated activation of YUCCA8 wxpression integrates remperature into the auxin pathway in regulating Arabidopsis hypocotyl growth. PLoS Genetics *8*, e1002594.

Sun, Q., Wang, S., Xu, G., Kang, X., Zhang, M., and Ni, M. (2019). SHB1 and CCA1 interaction desensitizes light responses and enhances thermomorphogenesis. Nature Communications *10*, 3110.

Thines, B., and Harmon, F.G. (2010). Ambient temperature response establishes ELF3 as a required component of the core Arabidopsis circadian clock. Proceedings of the National Academy of Sciences *107*, 3257-3262.

Tong, M., Lee, K., Ezer, D., Cortijo, S., Jung, J., Charoensawan, V., Box, M.S., Jaeger, K.E., Takahashi, N., Mas, P., *et al.* (2020). The Evening Complex

establishes repressive chromatin domains via H2A.Z deposition. Plant Physiology *182*, 612-625.

Wang, L., Fujiwara, S., and Somers, D.E. (2010). PRR5 regulates phosphorylation, nuclear import and subnuclear localization of TOC1 in the Arabidopsis circadian clock. The EMBO Journal *29*, 1903-1915.

Wei, X., Wang, W., Xu, P., Wang, W., Guo, T., Kou, S., Liu, M., Niu, Y., Yang, H.-Q., and Mao, Z. (2021). Phytochrome B interacts with SWC6 and ARP6 to regulate H2A.Z deposition and photomorphogensis in Arabidopsis. Journal of Integrative Plant Biology *63*, 1133-1146.

Xue, M., Zhang, H., Zhao, F., Zhao, T., Li, H., and Jiang, D. (2021). The INO80 chromatin remodeling complex promotes thermomorphogenesis by connecting H2A.Z eviction and active transcription in Arabidopsis. Molecular Plant *14*, 1799-1813.

Yakir, E., Hilman, D., Kron, I., Hassidim, M., Melamed-Book, N., and Green, R.M. (2009). Posttranslational regulation of CIRCADIAN CLOCK ASSOCIATED1 in the circadian oscillator of Arabidopsis. Plant Physiology *150*, 844-857.

Yamamoto, Y., Sato, E., Shimizu, T., Nakamich, N., Sato, S., Kato, T., Tabata, S., Nagatani, A., Yamashino, T., and Mizuno, T. (2003). Comparative genetic studies on the APRR5 and APRR7 genes belonging to the APRR1/TOC1 quintet implicated in circadian rhythm, control of flowering time, and early photomorphogenesis. Plant and Cell Physiology *44*, 1119-1130.

Yamashino, T., Matsushika, A., Fujimori, T., Sato, S., Kato, T., Tabata, S., and Mizuno, T. (2003). A link between circadian-controlled bHLH factors and the APRR1/TOC1 quintet in Arabidopsis thaliana. Plant and Cell Physiology *44*, 619-629.

Yoo, S.-D., Cho, Y.-H., and Sheen, J. (2007). Arabidopsis mesophyll protoplasts: a versatile cell system for transient gene expression analysis. Nature Protocols *2*, 1565.

Zhang, L.-L., Shao, Y.-J., Ding, L., Wang, M.-J., Davis, S., and Liu, J.-X. (2021). XBAT31 regulates thermoresponsive hypocotyl growth through mediating degradation of the thermosensor ELF3 in Arabidopsis. Science Advances *7*, eabf4427.

Zhang, Y., Liu, T., Meyer, C.A., Eeckhoute, J., Johnson, D.S., Bernstein, B.E., Nusbaum, C., Myers, R.M., Brown, M., Li, W., *et al.* (2008). Model-based Analysis of ChIP-Seq (MACS). Genome Biology *9*, R137.

Zhao, H., and Bao, Y. (2021). PIF4: Integrator of light and temperature cues in plant growth. Plant Science, 111086.

Zhu, J.-Y., Oh, E., Wang, T., and Wang, Z.-Y. (2016). TOC1–PIF4 interaction mediates the circadian gating of thermoresponsive growth in Arabidopsis. Nature Communications *7*, 13692.

ABSTRACT IN KOREAN (국문 초록)

생체시계는 주위 환경의 빛의 순환에 의해 만들어진 후 생장과 발달, 방어기작 등의 식물의 일주기적 생리활성을 조절한다. 본 연구에서는 밤에 활성을 가지는 식물 생체시계 구성인자 PSEUDO RESPONSE REGULATOR 5 (PRR5)와 TIMING OF CAB EXPRESSION 1 (TOC1)이 Evening Complex (EC)의 구성인자 EARLY FLOWERING 3 (ELF3)와 상호작용을 통해 *PHYTOCHROME INTERACTING FACTOR 4* (*PIF4*) 유전자의 발현을 조절하여 일주기적 하배축 생장을 조절하는 기작을 밝혔다. 세 유전자의 돌연변이 *prr5 toc1 elf3* 식물의 밤 사이에 생장 속도와 *PIF4* 유전자 발현이 급격하게 증가하는 것을 보아 이들 유전자는 밤 사이의 하배축 생장을 상승적으로 억제함을 확인하였다. 특히 밤 시간 동안의 PRR5, TOC1, ELF3 단백질의 *PIF4* 발현 억제는 염색질 리모델링을 일으키는 SWI2/SNF2-RELATED (SWR1) 복합체와 함께 상호작용하여 *PIF4* 유전자 지역에 H2A.Z 뉴클레오솜을 삽입함으로써 이뤄지는 것을 확인했다. 결과적으로 본 연구는 PRRs-EC-SWR1 복합체에 의한 후성유전학적 조절을 통해 일주기적 하배축 생장이 조절되는 메커니즘을 밝힌다.

주요어 : 하배축 생장, 생체시계, PRR, Evening Complex (EC), H2A.Z, SWR1 복합체, PIF4
학번 : 2019-22185